j mater res technol. 2016;xxx(xx):xxx–xxx

Available online at www.sciencedirect.com

jmr&t Journal of Materials Research and Technology

www.jmrt.com.br

Original Article

A potential attenuation equation for cathodically polarized pipelines and risers

Roland Tolulope Loto[a,c,*], *Roy Olakunle Loto*[b], *Cleophas Akintoye Loto*[a]

[a] *Department of Mechanical Engineering, Covenant University, Ota, Ogun State, Nigeria*
[b] *Department of Metallurgical and Materials Engineering, University of Lagos, Akoka, Lagos, Nigeria*
[c] *Department of Chemical, Metallurgical & Materials Engineering, Tshwane University of Technology, Pretoria, South Africa*

ARTICLE INFO

Article history:
Received 14 January 2016
Accepted 21 May 2016
Available online xxx

Keywords:
Alloys
Corrosion resistance
Cathodic polarization
Electrochemical property
Coatings

ABSTRACT

The cathodic protection system analysis as tools for one-dimensional pipelines and risers was modeled and derived incorporating the relevant resistance terms. The new expression pertains to pipelines with superimposed anodes. Comparisons were made between the potential attenuation projected by the new expression, the classical equation of Uhlig and the boundary element modeling technique. It was confirmed that the newly derived equation is more conservative than the boundary element modeling technique due to its consideration of the metallic path resistance and the Uhlig equation because of its consideration of the anode resistance.

1. Introduction

Pipelines are generally recognized as the safest, most efficient and cost effective means of transportation for oil and gas from fixed production facilities [1]. Structural and high strength steels are the most commonly used materials for the construction of marine petroleum transport pipelines as well as buried onshore pipelines [2]. However, it suffers from an inherent lack of corrosion resistance in an electrolyte such as soil or seawater. This requires that in order to prevent pipeline failure due to corrosion, corrosion control systems have to be designed and maintained such that a high degree of reliability is realized [3]. The issue of reliability is even more important in the case of deep-water installations. Several publications [4–6] indicate that the major cause of failure in pipelines has been corrosion. Minerals management date (MMS) data states that over 50% of failures in marine pipelines to this mode. Approximately 63% of the cases have occurred on pipelines as opposed to risers and 69% resulted from external as opposed to internal corrosion. At the same time, 88% of the external corrosion occurred on risers while 12% were on pipelines [7].

Cathodic protections combined with the use of coatings are the major source of protection for offshore and buried onshore pipelines [8,9]. It has historically been employed as the corrosion control methodology for the submerged

* *Corresponding author.*
E-mail: tolu.loto@gmail.com (R.T. Loto).
http://dx.doi.org/10.1016/j.jmrt.2016.05.008

Please cite this article in press as: Loto RT, et al. A potential attenuation equation for cathodically polarized pipelines and risers. J Mater Res Technol. 2016. http://dx.doi.org/10.1016/j.jmrt.2016.05.008

portion of petroleum production platforms [10,11]. However, the one-dimensional nature of pipelines entails the use of coatings combined with cathodic protection. In the former case (petroleum production platforms), the fundamental parameters important in cathodic protection design are the anode resistance and structure current density demand. On the other hand, for metallic pipelines, the coating quality and metallic path resistance must be taken into account from a general point of view. Cathodic protection systems can be of the impressed current type or the galvanic anode type [12–15]. Impressed current cathodic protection (iccp) systems are mainly used for buried onshore pipelines but not feasible for offshore pipelines. In both cases the limiting distance to which the corrosion protection can be effected is a function of the voltage drop along the metallic pipeline, which arises in conjunction with the current return to ground. Another factor that affects the distance to which corrosion protection is afforded is the quality of the protective coating. Thus, the higher the coating quality, the less the current demand of the pipe and, as a result, the less the voltage drop for a pipeline of a given length. However, coating quality of marine pipelines is considerably less than that of buried onshore counterparts so that this distance of protection is considerably less in the former case than in the latter. To maximize the distance, to which protection is achieved, the region of the pipeline near the rectifier and anode may be overprotected [16,17]. This can cause coating damage in the form of blistering and disbondment, which in turn increases the pipe current demand. Because of these factors, corrosion control of the majority of marine pipelines is provided by galvanic anodes, i.e., galvanic anode cathodic protection (gacp). This is invariably of the bracelet type for structural, economic and installation considerations.

The design normally assumes a certain percentage of coating bare area and employs galvanic bracelet anodes spaced about 250 m apart. This relatively short spacing emanates because of the limitations on the size of the bracelet anodes that can be deployed from a lay barge and the fact that the current density demand is relatively high and service lives of 25–30 years are needed. For the buried onshore pipeline on the other hand, the higher coating quality combined with the iccp system is such that the metallic path ground return resistance is the controlling factor and as a result the anode ground bed spacing of 50–100 km can be realized [18].

For offshore pipelines with closely spaced galvanic anodes, common on new installations, the metallic path resistance is negligible and the design process has historically involved the following steps [19,20]:

(1) Calculation of the net pipe current demand from the expression:

$$I_c = A_c * f_c * i_c \tag{1}$$

where I_c is the net pipe current density demand [21], A_c is the pipe surface area, f_c is the coating breakdown factor (the ratio of bare area to total pipe surface area), i_c is the current density demand.

(2) Determination of the total anode mass (kg) required from a modified form of Faraday's law

$$M = \frac{8760 i_m \cdot T}{u \cdot C} \tag{2}$$

where T is the design life (years), C is the current capacity of an individual anode (A h/kg), u is the utilization factor, i_m is the mean current density to polarize the pipeline.

8760 h in 365 days. Finally, the number of anodes, N, is determined as shown below;

$$N = \frac{I_a}{i_a} \tag{3}$$

where I_a is the total current required and i_a is the current output from an individual anode.

However, for marine pipeline cp retrofits, marine pipelines deployed by reeling with subsequent anode sled placement, buried onshore pipelines with iccp systems, anode spacing as mentioned above, is likely to be large and metallic path resistance significant. For these situations, numerical methods such as boundary element modeling (BEM) are commonly used; first principles based equations of Morgan and Uhlig are also used [22,23]. These equations are used to project the potential attenuation along the pipeline in order to determine the polarization at any point along the pipeline. This therefore enables the calculation of the protection distance of the cathodic protection system along the pipeline, which in turn enables the determination of a conservative anode spacing, which will provide the desired protection economically. They are also used to calculate the anode current output, which helps in calculating the life span of the anode (in case of gacp system), or the current consumption (in the case of iccp system). With the Morgan's equation and also the Uhlig's equation, anode resistance is not taken into consideration and there are levels of uncertainty associated with the calculated magnitude of polarization at the drainage point, the mid-anode spacing and at a variable point z from a drainage point. There are also levels of uncertainty associated with the current density demand projected by the equation.

The BEM on the other hand incorporates anode resistance and expresses the closed circuit cathode potential as a function of distance from the drainage point but it does not accommodate the metallic path resistance [21]. Hence it predicts a constant polarization beyond the field of the anode whereas, theoretically given the fact that the pipeline has a finite resistivity, the polarization will decrease with distance. It is therefore possible for the polarization at some point to have risen above $-0.80\,V_{AgCl}$ with the BEM projecting a significantly higher value [24,25]. This means that there are situations where the potential at a point along the pipeline is affected by all four resistance terms earlier described. Using any of these methods would give results that incorporate some amount of error. In light of the limitations of the methods described, this research aims to derive a first principle based attenuation equation that incorporates all the four resistance terms (anode resistance, coating resistance, polarization resistance and metallic path resistance). This is to accurately calculate

Please cite this article in press as: Loto RT, et al. A potential attenuation equation for cathodically polarized pipelines and risers. J Mater Res Technol. 2016. http://dx.doi.org/10.1016/j.jmrt.2016.05.008

the pipeline polarization behavior and the pipe current demand.

2. Methodology

The modeling research was carried out in two parts: (i) development of an inclusive potential attenuation model for pipeline cathodic protection and (ii) verification of the attenuation model.

2.1. *Development of an inclusive potential attenuation model for pipeline cathodic*

2.1.1. *Protection*

According to Pierson et al. [26], the electrode (pipeline or riser) potential can be represented as the charge gradient associated with an electric double layer or

$$E_c(z) = E_m(z) - E_e(z) + K_{ref} \tag{4}$$

where $E_m(z)$ and $E_e(z)$ are the potentials of the metallic pipe and electrolyte respectively, at a distance z from the drainage point of an offset anode or the centreline of an anode superimposed on the pipeline in which the anodes are identical and equally spaced and K_{ref} (constant) is the potential of the reference electrode. In addition,

$$\eta_c(z) = E_c(z) - E_{corr} \tag{5}$$

where E_{corr} is the free corrosion potential and $\eta_c(z)$ is the degree of polarization from the free corrosion potential. By taking the second derivative of Eqs. (4) and (5) and substituting for $E_c(z)$ the expression below is obtained.

$$\eta_c''(z) = E_m''(z) - E_e''(z) \tag{6}$$

The method adopted was to derive a mathematical expression for the three component terms as shown in Eq. (6).

2.2. *Expression for cathodic polarization*

The $\eta_c(z)$ term was assumed for simplicity to have a linear relationship with the current density $i_c(z)$ as

$$\eta_c(z) = \frac{\alpha}{f} \cdot i_c(z) \tag{7}$$

where α is the polarization resistance, f is the coating breakdown factor, $i_c(z)$ is the current density at point z along the pipeline.

2.3. *Expression for electrolyte potential variation*

The expression for $E_e(z)$ was developed by considering a pipeline, which is protected by a spherical anode of radius r_a located at an offset distance y_{of} from the pipeline. A spherical anode was assumed for mathematical simplicity although, in reality, bracelet anodes are used for marine pipelines or anode sled in the case of retrofits. However, the effect of the geometry on the cathodic protection system is negligible if the resistance to remote earth of the bracelet anode and the sphere anode are the same. Therefore, the equivalent sphere anode for a given bracelet anode can be calculated by referring to McCoy's formula [27]. For a bracelet anode of a given surface area, the approximate resistance to remote earth is given by McCoy's formula as

$$R = \frac{0.315\rho_e}{\sqrt{A}} \tag{8}$$

where ρ_e is the resistivity of the electrolyte, A is the exposed surface area of the bracelet anode. By assuming a sphere of the same surface area to the bracelet anode, the equivalent sphere radius $r_a(eq)$ is calculated as

$$r_a(eq) = \sqrt{\frac{S_a}{4\pi}} \tag{9}$$

or

$$r_a(eq) = 0.282\sqrt{S_a} \tag{10}$$

where S_a is the sphere surface area.

$E_e(z)$ is considered to be the product of the resistance $R_e(z)$ between the anode and a radial outward distance d in the electrolyte and the net current in the electrolyte ($I_a(z)$) at that point in accordance with Ohm's law where $d \equiv \sqrt{z^2 + y_{of}^2}$

$$\text{i.e.} \quad E_e(z) = R_e(z) * I_a(z) \tag{11}$$

The potential difference between two points r_1 and r_2 is given by the classical equation for potential drop associated with a spherical electrode in an electrolyte of resistivity ρ_e as

$$\Delta E_{r_1 \to r_2} = -\int_{r_1}^{r_2} \beta_e dr = -\int_{r_1}^{r_2} \frac{\rho_e \cdot I}{4\pi r^2} dr = \frac{\rho_e \cdot I}{4\pi}\left[\frac{1}{r_1} - \frac{1}{r_2}\right] \tag{12}$$

where β_e is the electric field intensity and I is the total current discharged by the anode. Thus, upon substituting r_1 with r_a and r_2 with $(y_{of}^2 + z_2)^{1/2}$ and dividing the resulting expression by I, the resistance between the anode surface and a radial outward distance d, $R_e(z)$ was obtained as

$$R_e(z) = \frac{\rho_e}{4\pi}\left[\frac{1}{r_a} - \frac{1}{(y_{of}^2 + z_2)^{1/2}}\right] \tag{13}$$

An expression for $I_a(z)$ was obtained by considering the region Ψ in Fig. 1, which encompasses the entire current field of the anode. Where anodes are equally spaced, the region will intersect the pipeline at the midpoint between the anodes (i.e. $z = L$ where L is the semi-anode spacing). Since there is conservation of charge, the net current passing through a planar surface perpendicular to the pipeline at $z = z_1$, $I_a(z_1)$ was assumed to adhere to the expression

$$I_e(z_1) = I_p(z_1) = 2\pi r_p \int_{z_1}^{L} i_c(z)dz \tag{14}$$

where $I_p(z_1)$ is the total current entering the pipe between the points z_1 and L on the pipe or the net current flowing to the

Please cite this article in press as: Loto RT, et al. A potential attenuation equation for cathodically polarized pipelines and risers. J Mater Res Technol. 2016. http://dx.doi.org/10.1016/j.jmrt.2016.05.008

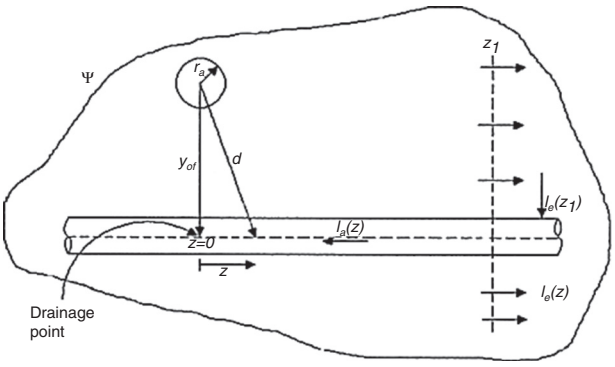

Fig. 1 – Current field and individual current elements of an offset galvanic anode associated with a pipe.

anode at z_1, $i_c(z)$ is the cathode (pipe) current density and r_p is metallic pipe outer radius. The net current in the electrolyte at z_1, $I_a(z_1)$ is double that of $I_e(z_1)$ due to the contribution from both sides of the anode i.e.

$$I_a(z_1) = 2I_p(z_1) = 4\pi r_p \cdot \int_{z_1}^{L} i_c(z)dz \tag{15}$$

Due to the coating on the pipeline, the bare portion is significantly smaller than in a situation where there is no coating at all. This was exposed with the coating breakdown factor *f*, which is the fraction of the pipeline that is bare (i.e. not coated). At the same time, some parts of the bare portion are anodic sites while others are cathodic sites. When the pipeline is polarized, the anodic reaction (on the anodic sites) would have been suppressed and the cathodic reaction (on the local cathodic sites) will be accelerated. It was assumed that on the basis of this, current from the anode enters the pipeline at the local sites hence the current density term in Eqs. (14) and (15) was the current density of the local cathodic sites of the bare portion. This made necessary to evaluate the area of the local cathodic sites for a given bare portion (because the local anodic area usually differs from the local cathodic area in size). This was done by deriving the following expressions from the combined activation polarization curve for the cathodically polarized metal.

$$i_d = i_e \exp\left(\frac{2.303\,(E_{corr} - E_e)}{b_c}\right) \tag{16}$$

$$i_{corr} = i_o \exp\left(\frac{2.303\,(E_{corr} - E_o)}{b_a}\right) \tag{17}$$

where i_d the current density is demand of the local cathodic sites and i_{corr} is the dissolution current density for the local anodic sites, b_c is the Tafel constant for the cathodic reaction and b_a is the Tafel constant for the anodic reaction. Eqs. (16) and (17) were re-written to express the area and absolute current of the local anodic and cathodic areas of the pipe.

$$i_d = A_c i_e \exp\left(\frac{2.303(E_{corr} - E_e)}{b_c}\right) \tag{18}$$

$$i_{corr} = A_a i_o \exp\left(\frac{2.303(E_{corr} - E_o)}{b_a}\right) \tag{19}$$

A_c is the electrode active surface area for the cathodic site, while A_a is the electrode active surface area for the anodic site. From literature, total anodic reaction is equal to total cathodic reaction; hence it was considered that for pipeline without a cathodic protection system (an unpolarized pipeline)

$$I_d = i_{corr} \tag{20}$$

From this expression [Eq. (20)], Eq. (21) was derived

$$A_{bc} = \frac{A_b}{\gamma} \tag{21}$$

where A_{bc} = area of exposed cathodic sites on the pipe metal, γ = ratio of total pipe surface area to area of exposed cathodic sites on the pipe metal, A_b = total pipe surface area.

$$\gamma = \frac{i_e \exp((2.303(E_{corr} - E_e))/b_c)}{i_o \exp((2.303(E_{corr} - E_o))/b_a)} + 1 \tag{22}$$

Eq. (15) was then rewritten in terms of the area of the local cathodic sites of the bare portion and the coating breakdown factor.

$$I_a(z) = 2I_p(z) = \frac{4\pi r_p \cdot f}{\gamma} \cdot \int_{z}^{L} i_c(z)dz \tag{23}$$

$I_a(z)$ was substituted with $I_c(z)$ using Eq. (23) and $R_e(z)$ was also substituted using Eq. (11). Upon differentiating the product of the resulting equations twice (to obtain the second differential of $[I_a(z) \cdot R_e(z)]$), the expression of $E''_e(z)$ was obtained to be

$$E''_e(z) = \frac{\rho_e \cdot r_p \cdot f}{\gamma}\left[d\left(\frac{d^2 - 3z^2}{d^5}\right) \cdot \int_{z}^{L} i_c(z)dz + \left(\frac{1}{r_a} - \frac{1}{d}\right) i'_c(z) + \frac{z}{d^3} i_c(z)\right] \tag{24}$$

2.4. *Expression for metallic pipe potential variation*

Ohm's law was again taken into consideration in deriving an expression for $E_m(z)$. According to Ohm's law; the potential change along a pipe at a point z is given by

$$\frac{\partial E_m}{\partial z} = -R_m \cdot I_p(z) \tag{25}$$

Given the fact that R_m is constant, $E''_m(z)$ was obtained by combining the above expression with Eqs. (23) and (6) after which it was differentiated twice to obtain

$$E''_m(z) = \frac{2\pi f \cdot r_p \cdot R_m \cdot i_c(z)}{\gamma} \tag{26}$$

2.5. *The governing equation*

The expressions for the electrolytic and metallic potential gradient along the pipeline [Eqs. (24) and (26)] were substituted into Eq. (6) then $i_c(z)$ substituted with $\eta_c(z)$ according

Please cite this article in press as: Loto RT, et al. A potential attenuation equation for cathodically polarized pipelines and risers. J Mater Res Technol. 2016. http://dx.doi.org/10.1016/j.jmrt.2016.05.008

to Eq. (7). The terms were brought together and rearranged thus providing an expression for the potential attenuation along a pipeline as:

$$\eta_c(z) = \left[\eta_c''(z) + \frac{\rho_e \cdot r_p}{k}\left(\left(\frac{1}{r_a} - \frac{1}{d}\right)\eta_c'(z) + d\left(\frac{d^2 - 3z^2}{d^5}\right)\cdot\int_z^L \eta_c(z)dz\right)\right]\cdot\left[\frac{r_p}{k}\left(2\pi R_m - \frac{2z\cdot\rho_e}{d^3}\right)\right] \quad (27)$$

where

$$k = \frac{\alpha\cdot\gamma}{f} \quad (28)$$

k is the effectual coating resistivity.

Eq. (27) holds for the pipe with length between $z = r_a$ and $z = L$ for pipelines protected by superimposed anodes and for the entire pipe length for pipelines protected by displaced anodes. For superimposed anodes however, only the portion between $z = l_a$ and $z = L$ is required to be calculated; where l_a is the real anode's length (length of the bracelet anode for instance). This is because the region between $z = 0$ and $z = l_a$ in the case of pipelines protected by superimposed nodes is covered by the anode and therefore is not exposed to the electrolyte, hence it does not corrode.

There was no solution known to Eq. (27), thus it was solved numerically using an explicit finite difference scheme that is based upon first and second derivatives in space [28]. The first derivative was represented by backward finite difference

$$\frac{\partial\eta}{\partial z} = \frac{\eta_i^{m+1} - \eta_{i-1}^{m+1}}{\partial z} \quad (29)$$

and the second derivative by

$$\frac{\partial^2\eta}{\partial^2 z} = \frac{\eta_{i+1}^{m} - 2\eta_i^{m+1} + \eta_{i-1}^{m+1}}{\partial^2 z} \quad (30)$$

Eqs. (28) and (29) were substituted into Eq. (27) to yield

$$\eta_i^{m+1} = \frac{(-QHdz/2)(\sum_{j=1}^{N-1} 2\eta_{i+j}^{m} + \eta_N^{m}) + (\eta_{i-1}^{m+1}/dz)H((1/r_a) - (1/d_i)) - (\eta_{i-1}^{m+1}/\partial z^2) - (\eta_{i+1}^{m}/\partial z^2)}{(-2/\partial z^2) + (H/dz)((1/r_a) - (1/d_i)) + ((2z_iH/d_i^3) + B) + (QHdz/2)} \quad (31)$$

where

$$Q = d\left(\frac{d^2 - 3z^2}{d^5}\right) \quad (32)$$

$$H = \frac{\rho_e\cdot r_p}{k} \quad (33)$$

$$B = \frac{2\pi r_p\cdot R_m}{k} \quad (34)$$

where n is the number of nodes on the cathode between the anode surface and midpoint (the number of elements of length dz plus 1), m is the iteration step and i refers to the internal node over the length of the cathode between the anode surface and the midpoint. Eq. (30) provided an explicit means for calculating the cathode polarization at each internal node for the next iteration step (iteration step $m+1$) based on the values of the present iteration step (iteration step m) at the nodes.

The representation of the boundary conditions at the end nodes was done using

$$\eta_c(z = 0) = E_a - E_{corr} = \eta_a \quad (35)$$

At the beginning (i.e. the anode)

$$\left.\frac{\partial\eta_c(z)}{\partial z}\right|_{z=L} = 0 \quad (36)$$

At the midpoint between the anodes, the derivative boundary condition is represented as

$$\eta_{i=1}^{m+1} = \frac{4\cdot\eta_{i=n-1}^{m+1} - \eta_{i=n-2}^{m+1}}{3} \quad (37)$$

The element closest to the anode $\eta_{i=0}$ was considered to be equal to η_a. Based on the anode polarization according to Eq. (34), η_a was also assigned to every element discretizing the cathode for the initial iteration step $m = 1$ as an initial estimate. The iteration succession was ended when $\Delta\eta_{rms}$ became less than 10^{-9}. The true solution of potential attenuation along a cathodically polarized pipeline is difficult and expensive to measure in situ, hence the validity of the proposed model was determined by comparison with alternative modeling techniques – boundary element modeling (BEM) and Uhlig's equation under conditions where they were considered accurate.

2.6. *Verification of the potential attenuation model*

2.6.1. *The effect of parameter k and anode spacing on the potential attenuation*

The attenuation model [Eq. (27)] was compared with alternative modeling techniques – BEM and Uhlig's equation. Comparisons were for k values of 4, 20, 100 and 1000 $\Omega\,m^2$ for a hypothetical pipe. This covers the range for a pipeline, which is very difficult to polarize, to that which is likely to be met in practice. Other parameters for the hypothetical system are listed in Table 1. The potential attenuation along the pipeline obtained by these three methods for each value of k was plotted as a function of distance along the pipeline from the anode (i.e. as a function of z) to verify the accuracy of Eq. (27).

Using the same parameters in Table 1 for $k = 100\,\Omega\,m^2$ but with $L = 3000$ m, the attenuation profiles from BEM and Eq. (27), neglecting metallic path resistance (i.e. assuming $\rho_m = 0$), were plotted. This was done to show the effect of the metallic path resistance, which is not considered by the BEM, on the polarization of a pipeline in situations where it is not negligible. By relating $\eta_c(z)$ to the current density demand of the pipe, the anode current output was determined by Eq. (27) using the pipe and electrolyte parameters that are in Table 1 and the

Please cite this article in press as: Loto RT, et al. A potential attenuation equation for cathodically polarized pipelines and risers. J Mater Res Technol. 2016. http://dx.doi.org/10.1016/j.jmrt.2016.05.008

Table 1 – Pipeline and electrolyte parameters for a hypothetical system used in analysis [27].

Pipe/CP parameter	Example
Pipeline outer radius, m	0.136
Pipeline inner radius, m	0.128
Anode spacing (2 L), m	244
Coating breakdown factor	0.04
Equivalent sphere radius of anode, m	0.201
Electrolyte resistivity, Ω m	0.30
Pipe resistivity, Ω m	1.7×10^{-9}
Free corrosion pipe potential, $V_{Ag/AgCl}$	−0.65
Anode potential, $V_{Ag/AgCl}$	−1.05

result obtained was plotted against k. The results obtained for the Uhlig equation and the BEM were also plotted on the same graph for comparison.

2.6.2. *The effect of pipe current demand and anode separation distance upon*

2.6.2.1. Potential attenuation and anode current output. The attenuation profiles for one-half anode spacing of 1000, 2000 and 3000 m with $k = 100\ \Omega\ m^2$ and also for one-half anode spacing of 2000, 6000, and 10,000 m with $k = 1000\ \Omega\ m^2$ using the pipe and environment parameters in Table 1, as obtained from Eq. (27) under the above conditions, were also plotted as a function of one-half anode spacing in order to investigate the accuracy of the anode current output projected by Eq. (27).

To further compare Eq. (27) to the BEM, a plot of the potential difference between BEM and Eq. (27) at the mid-anode point as a function of k was made for various anode spacing ranging from 250 to 10,000 m using the pipe and electrolyte parameters in Table 1. The percentage difference between the anode current outputs calculated using the BEM and Eq. (27) was also plotted against k for various anode spacing ranging from 250 to 10,000 m.

2.6.3. *Effect of offset distance upon potential attenuation along a pipeline*

Eq. (27) was compared with the BEM for a situation where a pipeline is protected by offset anodes. This is the case in practice when a pipeline is protected by an anode array such as in the case of retrofits. Plots of pipe potential versus distance from drainage were obtained from Eq. (27) and BEM using the parameters in Table 1, except with $r_a = 0.170$ m, $\rho_e = 0.15$ and 1 Ω m, k values of 100 and 1000 $\Omega\ m^2$, anode spacings of 200, 500, 1000, 2000 m, and y_{of} values of 1, 5 and 10 m.

When using offset anodes, the anode potential and the drainage point potential are different so the drainage point potential was calculated using classical equation for potential drop and associated with a spherical anode in an electrolyte

$$\Delta E_{r_a \to y_{of}} = \frac{\rho_e \cdot I}{4\pi}\left[\frac{1}{r_a} - \frac{1}{y_{of}}\right] \tag{38}$$

where I_a is the anode current output and r_a(eq) is the radius of the equivalent anode.

The anode current output was obtained by calculating it for a situation where the same anode was superimposed on the pipeline (since it would be the same as in the case of an offset anode). However, in the case of displaced anodes, no part of the pipeline was covered by the anode. Thus the pipeline is completely exposed to the electrolyte. Hence, when initially calculating the anode current by first assuming a superimposed anode, the value of r_a was added to the semi-anode spacing. This was done because Eq. (27) holds from $z = r_a$, hence, the results obtained would reflect the current demand by the entire pipe not excluding the region covered by the anode (since the distance between $z = r_a$ and $z = L + r_a$ is equal to that between $z = 0$ and $z = L$). The value obtained was then substituted into Eq. (38).

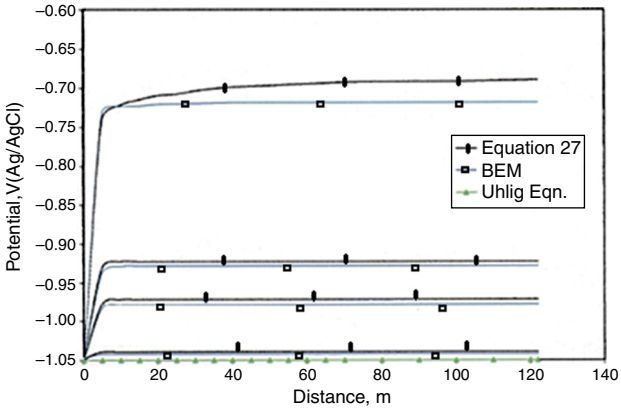

Fig. 2 – Comparison of potential profiles projected by Eq. (27), BEM and Uhlig's equation.

3. Results and analysis

Eq. (38) was compared to the boundary element modeling (BEM) and Uhlig's equation in order to verify its accuracy. The comparison was made by looking into the potential projected by the three equations under various conditions. The conditions included various combinations of polarization resistance, anode spacing, offset distance and pipe current demand. The anode current output (I_a), calculated from these three equations under some of the above conditions, were also compared.

3.1. *Effect of polarization resistance and anode spacing potential attenuation*

Fig. 2 presents a plot of pipe potential as a function of distance from an anode surface determined from the Uhlig equation, boundary element modeling and Eq. (27) for k values of 4, 20, 100 and 1000 $\Omega\ m^2$ in ascending order for a hypothetical pipe. Other pipe parameters are listed in Table 1.

Under the above conditions, it was observed that the Uhlig equation is relatively insensitive to polarization resistance and the current density demand of the pipe (the polarization resistance is equal to the current density demand). The Uhlig equation was also non-conservative when compared with BEM and Eq. (27) due to the fact that it predicts a greater cathodic polarization. The reason for this being that the Uhlig model does not take the anode resistance into consideration. The potential profile obtained from BEM and Eq. (27) was very close and hence in good mutual agreement with each other.

Please cite this article in press as: Loto RT, et al. A potential attenuation equation for cathodically polarized pipelines and risers. J Mater Res Technol. 2016. http://dx.doi.org/10.1016/j.jmrt.2016.05.008

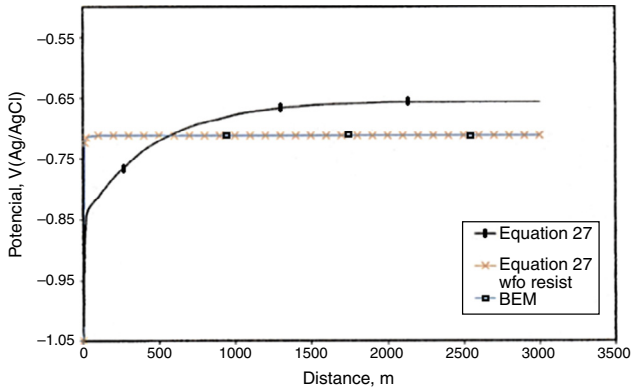

Fig. 3 – Comparison of potential projected by Eq. (27) and BEM where the former exhibits the presence and absence of the metallic path resistance term.

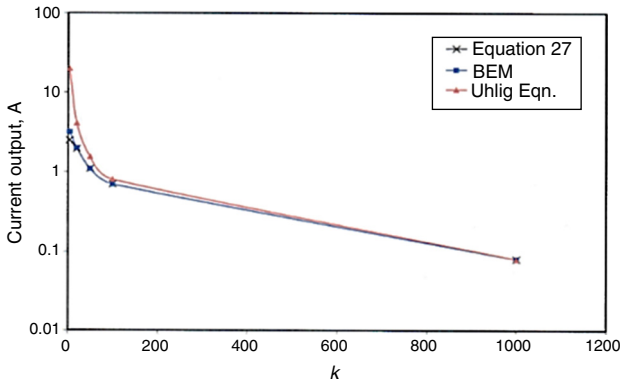

Fig. 4 – Comparison of anode current output as projected by Eq. (27), BEM and Uhlig's equation.

They featured a significant potential drop within roughly the first 10–15 m of the anode, the magnitude of which varied directly with the pipe current demand (i.e. polarization resistance and current demand). Beyond the field of the anode (the region where the anode resistance is influential), the potential for the remaining portion of the pipeline was relatively constant, although the potential drop in this region for Eq. (27) was slightly greater than that of BEM, the magnitude of this difference was inversely related to the current demand of the pipe. The reason for this is because of the inclusion of the metallic path resistance in Eq. (27) and its exclusion in BEM. In this situation, however, the difference between the potential profiles obtained from these two methods is not of any operative significance. It follows that since BEM is a proven technique for characterizing the potential field of a cathodically protected pipeline or riser, Eq. (27) is a viable means for projecting the potential attenuation along pipelines as well as anode current output.

Fig. 3 presents the potential attenuation profiles from (1) BEM, (2) Eq. (27), and (3) Eq. (27) neglecting metallic path resistance (i.e. assuming $\rho_m = 0$ in this case) for the same pipe and electrolyte parameters used in Fig. 2 with $k = 100\,\Omega\,m^2$ and $L = 3000$ m. E_c versus z for the three cases show a significant potential drop in the immediate vicinity of the anode. Beyond this region, the BEM and Eq. (27) without metallic path resistance exhibit a constant potential whereas Eq. (27) with metallic path resistance included is characterized by further potential attenuation along the length of the pipeline although of a much lesser magnitude. Hence, it follows that of the three equations, Eq. (27) with the metallic path resistance gave the most accurate presentation of the potential profile. Since Uhlig's equation does not take the anode resistance into consideration, it can be said to be non-conservative when the anode resistance is non-negligible and the BEM can also be said to be non-conservative where the metallic path resistance is non-negligible. Eq. (27) can be said to be the most accurate method for situations where both the metallic path resistance and anode resistance are significant.

Since the anode current output is a function of the potential, the current demand was determined from Eq. (27) for the same pipe and electrolyte parameters utilized in Fig. 2. Fig. 4 presents a plot of I_a against k as determined by Uhlig's expression, BEM and Eq. (27) based upon the same pipe and electrolyte parameters as Fig. 2. It shows that the anode current output projected by Eq. (27) and the BEM are very close to each other, i.e., they are in agreement. It is expected that the BEM will over-estimate the anode current output for longer pipe lengths where the metallic path resistance is not negligible (since the BEM over-estimates the potential in such situations). The Uhlig equation on the other hand clearly over-estimates the anode current output at very low values of polarization resistance (i.e. in the region of $k = 100\,\Omega\,m^2$) but more accurately at higher values of polarization resistance (around $k \geq 100\ \Omega\,m^2$). This was probably due to Uhlig equation neglecting the significant effect of the near-field at lower values of polarization resistance.

3.2. *The effect of pipe current demand and anode separation distance upon potential*

3.2.1. *Attenuation and anode current output*

Fig. 5 presents the attenuation profiles for different semi-anode spacing ranging from 1000 to 3000 m with $k = 100\,\Omega\,m^2$ projected by the BEM and Eq. (27) using the pipe and environment parameters in Table 1. Fig. 6 on the other hand

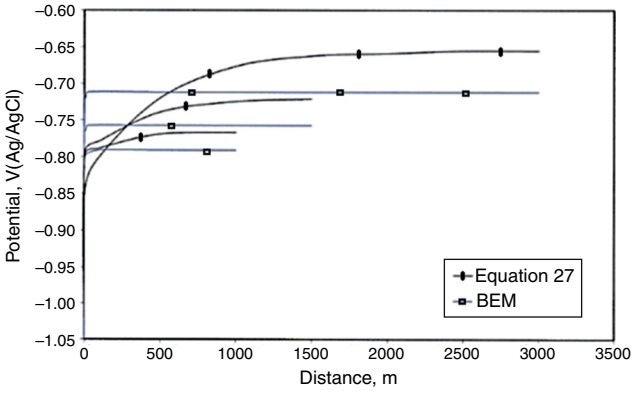

Fig. 5 – Comparison of potential profiles from Eq. (27) and BEM for pipelines with anode spacing from 1000 to 3000 m and $k = 100\,\Omega\,m^2$.

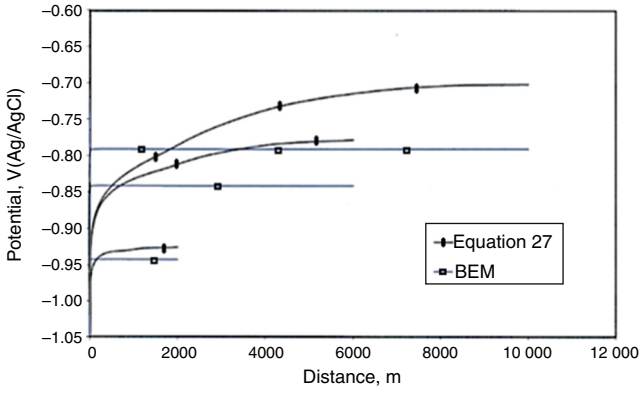

Fig. 6 – Comparison of potential profiles from Eq. (27) and BEM for pipelines with anode spacing from 2000 to 10,000 m and with $k = 1000\ \Omega\ m^2$.

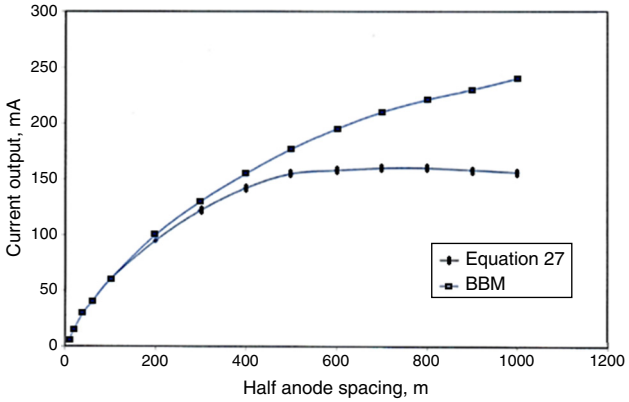

Fig. 8 – Anode current output as projected by Eq. (27) and BEM as a function of half anode spacing and for $k = 1000\ \Omega\ m^2$.

presents attenuation profiles for semi-anode spacing ranging from 1000 to 10,000 m with $k = 1000\ \Omega\ m^2$ projected by the same two methods.

Figs. 5 and 6 indicate that potential profiles projected by Eq. (27) is different from that projected by the BEM and the magnitude of this difference is directly proportional to (1) the distance from the anode (2) the semi-anode spacing and is inversely proportional to the polarization resistance. Eq. (27) is considered to be the more accurate of the two methods especially when the metallic path resistance is significant because it incorporates the term. It follows that on pipe for instance, the BEM can indicate protection along the entire length of the pipeline, whereas the pipe is under-protected beyond a certain point. Figs. 7 and 8 show the plots of anode current output as a function of semi-anode spacing for the same conditions used for Figs. 5 and 6, respectively. The plots show that the BEM and Eq. (27) are in good mutual agreement for relatively short spacing. However, for longer semi-anode spacing, the BEM projects that the current increases whereas, Eq. (27) projects that the current increases to a maximum and then decrease. The latter phenomenon is more prominent than the lower polarization resistance case. The lower anode current output projected by Eq. (27) in Figs. 7 and 8 compared with the BEM corresponds with the potential projected by the former in Figs. 5 and 6, which had a lesser magnitude. The difference is also due to the BEM not considering the metallic path resistance.

Fig. 9 presents a plot of difference in potential at the midpoint between the value projected by Eq. (27) and that projected by the BEM as a function of k for various anode spacing between 250 and 10,000 m. The curves show that, except for the largest anode spacing (10,000 m), the difference in potential increases with decreasing k. This trend arose due to the anode current output increasing with decreasing k with the BEM not accounting for the increasing voltage drop along the pipeline as a result of the increasing anode current output. However, a reverse trend was observed for $2L = 10{,}000$ m and $k < 600\ \Omega\ m^2$. This was due to the fact that as a result of the relatively low k and the large potential drop from the anode to the mid-anode point, the polarization at the midpoint was very small for both the BEM and Eq. (27) and the difference in potential projected by the two was small.

Fig. 10 presents the percentage difference in anode current output between the BEM and Eq. (27) as a function of k for the same anode spacing used in Fig. 9. It will be observed that, for all the values of anode spacing, the difference decreased with increasing value of k. This trend is particularly significant in

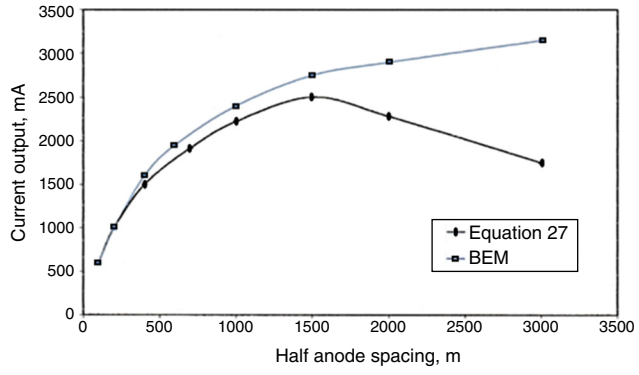

Fig. 7 – Anode current output as projected by Eq. (27) and BEM as a function of half anode spacing and for $k = 100\ \Omega\ m^2$.

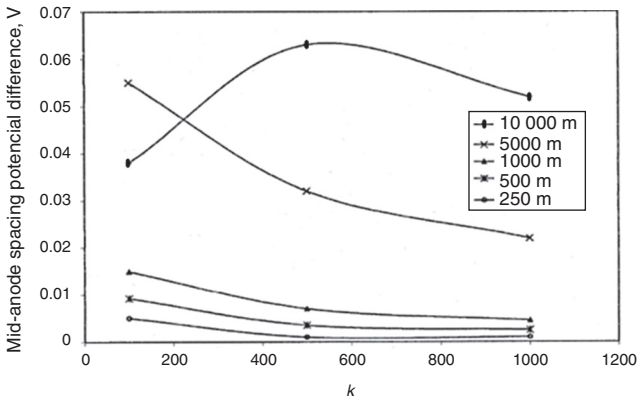

Fig. 9 – Plot of the difference between potential projected by Eq. (27) and BEM at the mid-anode point for different anode spacing as a function of k. A positive difference indicates a relatively positive potential projected by Eq. (27).

Please cite this article in press as: Loto RT, et al. A potential attenuation equation for cathodically polarized pipelines and risers. J Mater Res Technol. 2016. http://dx.doi.org/10.1016/j.jmrt.2016.05.008

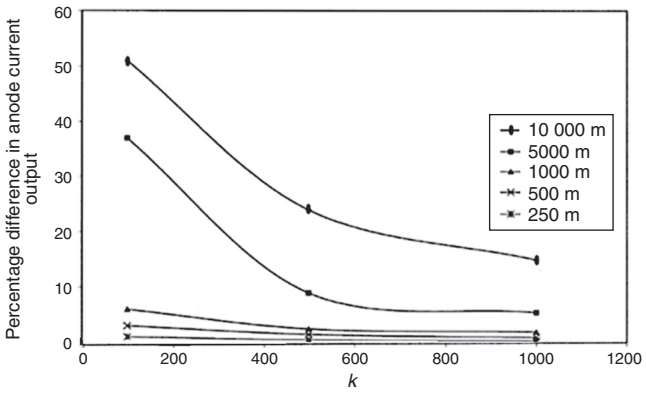

Fig. 10 – Plot of the percent difference in anode current output as projected by Eq. (27) and BEM as a function of k. A positive difference indicates relatively greater current projection by BEM.

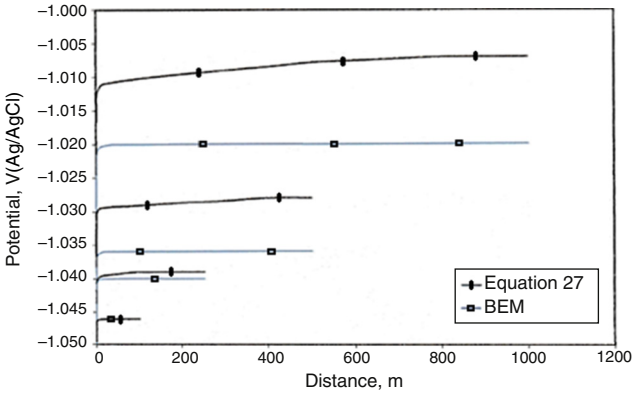

Fig. 12 – Potential attenuation profiles for a 0.272 m diameter pipeline with $\rho_e = 0.15\ \Omega$ m, $k = 100\ \Omega\ m^2$, and 0.340 m diameter equivalent spherical anode offset at 1 m, 5 m and 10 m.

the two largest anode spacing. This trend corresponds with Figs. 7 and 8 where the anode current output projected by the two methods differ with increase in anode space; the effect being greater the lower the value of k.

3.3. *Effect of offset distance upon potential attenuation along a pipeline*

Fig. 11 shows the potential attenuation profiles for y_{of} values at 1, 5 and 10 m with $\rho_e = 0.15$ and $k = 100\ \Omega\ m^2$, $r_a = 0.170$ m and anode spacings of 200, 500, 1000 and 2000 m as obtained from Eq. (27) and the BEM analysis. They all show exact similarities. The plots show that the BEM projects a larger polarization value along the pipeline than Eq. (27). The magnitude of the difference being directly proportional to the anode spacing. This difference is because of the BEM analysis neglects the metallic path resistance. The results also show that the greater the offset distance, the more positive the potential at $z = 0$ and the far field potential is essentially independent of the offset distance.

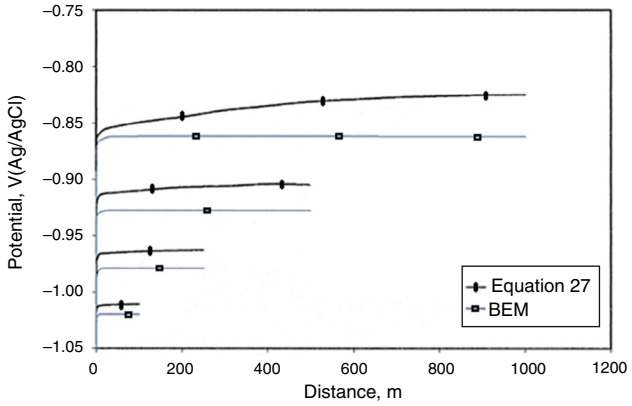

Fig. 11 – Potential attenuation profiles for a 0.272 m diameter pipeline with $\rho_e = 0.15\ \Omega$ m, $k = 100\ \Omega\ m^2$, and 0.340 m diameter equivalent spherical anode offset at 1 m, 5 m and 10 m.

Fig. 12 shows plots with the same parameters as Fig. 11 but with, $k = 1000\ \Omega\ m^2$. In comparison with the trend obtained in Fig. 11, it will be observed that (1) the attenuation in the immediate vicinity of the anode decreases with increasing polarization resistance, (2) the attenuation profile is more negative and (3) the protection distance is greater, thus the higher the polarization resistance.

The newly proposed equation can be used for pipeline cathodic protection design for (1) marine pipeline cathodic protection retrofits (2) buried onshore pipelines with impressed current cathodic protection systems and (3) marine pipelines deployed by reeling with subsequent anode sled placement where the metallic path resistance is significant. This is due to the fact that the newly proposed equation is more conservative than any of the other two methods mentioned in this situation and therefore more accurate.

4. Conclusion

A newly proposed potential attenuation equation for cathodically protected pipelines and risers was derived. The equation was solved using a finite difference method numerical procedure. The improved accuracy of this equation over the boundary element modeling (BEM) and the Uhlig equation is confirmed with example analysis provided. It was proven that the equation is in good agreement with the BEM when the metallic path resistance is negligible but more accurate in situations where there is finite value for the metallic path resistance. It was also shown to be more accurate than the Uhlig equation. The magnitude is proportional to the difficulty with which a pipeline is polarized.

Conflicts of interest

The authors declare no conflicts of interest.

Please cite this article in press as: Loto RT, et al. A potential attenuation equation for cathodically polarized pipelines and risers. J Mater Res Technol. 2016. http://dx.doi.org/10.1016/j.jmrt.2016.05.008

Acknowledgements

The authors acknowledge the Department of Metallurgical and Materials Engineering, Faculty of Engineering, University of Lagos, Akoka, Lagos, Nigeria and the Department of Mechanical Engineering, Covenant University, Ota, Ogun State, Nigeria for the provision of research facilities for this work.

REFERENCES

[1] Papavinasam S, Place T, Richter S. Managing corrosion of pipelines that transport crude oils. Pipeline Gas J 2013;240(3).
[2] Papavinasam S. Control in the oil and gas industry. USA: Elsevier Science & Technology; 2014. p. 133–77, http://dx.doi.org/10.1016/B978-0-12-397022-0.00003-0.
[3] Committee on the Safety of Marine Pipelines, Marine Board, National Research Council. Improving the safety of marine pipelines. Washington, DC: The National Academies Press; 1994 http://www.doc88.com/p-29024694714.html [16.04.15].
[4] Andersen T, Misund A. Pipeline reliability: an investigation of pipeline failure characteristics and analysis of pipeline failure rates for submarine and cross-country pipelines. J Pet Technol 1983:709.
[5] Analysis of the MMS pipeline leaks report for the Gulf of Mexico, Texaco, Santa Clara, Ventura, CA 93001, USA; 1985.
[6] Mandke JS. Corrosion causes most pipeline failures in the Gulf of Mexico. Oil Gas J 1990;8(44):40–4.
[7] Minerals management service data base, Gulf of Mexico Region, New Orleans, LA; 2015 http://www.gulfbase.org/organization/view.php?oid=mms [16.04.15].
[8] Cathodic protection; 2015 http://www.corrosionist.com/Corrosion_Control_Methods_Cathodic_Protection.htm [20.04.15].
[9] NACE International. Protecting underground pipelines from corrosion in sub-zero environments. ScienceDaily 2013 http://www.sciencedaily.com/releases/2013/10/131001124014.htm [04.05.15].
[10] Papavinasam S, Pannerselvam T, Doiron A. Applicability of cathodic protection for underground infrastructures operating at sub-zero temperatures. Corrosion 2013;69(9):936–45, http://dx.doi.org/10.5006/0881.
[11] Weiser J. Corrosion primer, protect underground piping from corrosion: what to do before the outage. Norton Corrosion Ltd.; 2015 http://www.nortoncorrosion.com/documents/cathodic-protection/Combined-Cycle-Outage-Handbook-2011.pdf [10.04.15].
[12] Cathodic protection; 2015 http://www.en.wikipedia.org/wiki/Cathodic_protection [14.04.15].
[13] Baxter R, Britton J. Offshore cathodic protection 101: what it is and how it works; 2015 http://cathodicprotection101.com/ [12.03.15].
[14] Bushman BJ. Galvanic anode, cathodic protection system design; 2013 http://www.bushman.cc/pdf/galvanic_anode_system_design.pdf [11.03.15].
[15] Types of cathodic protection systems; 2015 http://www.thegreenbook.com/cathodic-protection-systems.htm [11.02.15].
[16] Singh R. Corrosion control for offshore structures, cathodic protection and high efficiency coating. USA: Gulf Professional Publishing; 2014. p. 171.
[17] Bahadori A. Design considerations on cathodic protection for buried pipelines and marine structures, cathodic corrosion protection systems. In: A guide for oil and gas industries. USA: Gulf Professional Publishing; 2014. p. 91.
[18] Lysogorski DK, Hartt WH. A potential attenuation equation for design and analysis of pipeline cathodic protection systems with displaced anodes. Corrosion 2004;60(9):815–23.
[19] Cathodic Protection Design. DnV recommended practice RP401, Det Norske Veritas Industri Norge AS; 1993 http://www.scribd.com/doc/39861090/Nace-06102-New-Dnv-Cp-Code#scribd [11.01.15].
[20] Pipeline cathodic protection – part 2: cathodic protection of offshore pipelines, Working Document ISO/TC 67/SC 2 NP 14489. International Standards Organization; 1999.
[21] Morgan J. Cathodic protection. Macmillan; 1960. p. 140.
[22] Uhlig HH, Revie RW. Corrosion and corrosion control. 3rd ed. New York: John Wiley and Sons; 1985. p. 421.
[23] Hartt WH, Lysogorski DK. A first-principles based approach to potential attenuation projection for marine pipelines and risers; 2015 http://www.jcse.org/volume4/preprints/v4preprint11.txt [15.06.15].
[24] Britton J. Continuous surveys of cathodic protection system performance on buried pipelines in the Gulf of Mexico, paper no. 422 presented at CORROSION/92, Nashville, April 26–30; 1992.
[25] Corrosion control of steel-fixed offshore platforms associated with petroleum production. NACE Standard RP 0176. Houston: NACE; 1976.
[26] William HH, Lysogorski D, Qian H, Bethune K, Pierson P. Retrofit cathodic protection of marine pipelines associated with petroleum production; 2001 http://www.bsee.gov/Technology-and-Research/Technology-Assessment-Programs/Reports/200-299/242Ab/ [16.05.15].
[27] McCoy JE. Corrosion control by cathodic protection – theoretical and design concepts for marine applications. Inst Mar Eng Trans 1970;82:210.
[28] Chapra CS, Canale RP. Numerical methods for engineers. 2nd ed. New York: McGraw-Hill; 1988. p. 734.

Please cite this article in press as: Loto RT, et al. A potential attenuation equation for cathodically polarized pipelines and risers. J Mater Res Technol. 2016. http://dx.doi.org/10.1016/j.jmrt.2016.05.008